2012

In Vivo Demonstration of Surgical Task Assistance Using Miniature Robots

Jeff A. Hawks
University of Nebraska-Lincoln, jhawks2@unl.edu

Jacob Kunowski
University of Illinois at Urbana-Champaign, jacob.kunowski@gmail.com

Stephen R. Platt
University of Illinois at Urbana-Champaign, srplatt@illinois.edu

In Vivo Demonstration of Surgical Task Assistance Using Miniature Robots

Jeff A. Hawks*, Jacob Kunowski, and Stephen R. Platt

***Abstract*—Laparoscopy is beneficial to patients as measured by less painful recovery and an earlier return to functional health compared to conventional open surgery. However, laparoscopy requires the manipulation of long, slender tools from outside the patient's body. As a result, laparoscopy generally benefits only patients undergoing relatively simple procedures. An innovative approach to laparoscopy uses miniature *in vivo* robots that fit entirely inside the abdominal cavity. Our previous work demonstrated that a mobile, wireless robot platform can be successfully operated inside the abdominal cavity with different payloads (biopsy, camera, and physiological sensors). We hope that these robots are a step toward reducing the invasiveness of laparoscopy. The current study presents design details and results of laboratory and *in vivo* demonstrations of several new payload designs (clamping, cautery, and liquid delivery). Laboratory and *in vivo* cooperation demonstrations between multiple robots are also presented.**

***Index Terms*—*In vivo*, miniature, minimally invasive surgery (MIS), mobile, robotic surgery, wireless.**

I. Introduction

MINIMALLY invasive surgery (MIS) results in improved patient outcomes compared to conventional open surgical procedures [1]–[3]. Because the degree of patient trauma during surgery is directly related to the size and number of incisions, less invasive procedures reduce patient distress and recovery times compared to conventional open procedures [4]. Laparoscopy is MIS performed in the abdominal cavity using long, slender tools inserted through small tool ports. Laparoscopic surgery is difficult and imposes significant constraints on the surgeon, such as ergonomic limitations, reduced dexterity, and limited perception compared to conventional open surgery [5], [6].

Surgical robotic systems are aimed at mitigating these limitations. Robots such as the da Vinci Surgical System include tremor reduction, additional articulations in surgical instruments, stereoscopic vision, corrections for motion reversal, and motion scaling [7]–[9]. Recent improvements in the da Vinci Surgical System have focused on reducing setup time and improving visualization [10]. However, dexterity limitations imposed by the tool ports still exist because robots such as da Vinci remain located outside the patient. Furthermore, da Vinci is expensive, cumbersome, and requires significant operating space [11], [12].

The ARES system developed by Harada *et al*. [13] requires assembly after insertion and does not feature a wheeled robotic platform. Robots for single port surgery developed through the ARAKNES project [14], Wortman *et al*. [15], and Ding *et al*. [16] are confined to the incision location. Our study [17], [18] focuses on the development of miniature, inexpensive robots that are intended to be inserted entirely into the abdominal cavity through a single incision. Once inside the patient, these wireless robots can be maneuvered to an injury site away from the incision.

This paper presents the design and demonstration of three payload variations: clamping, cautery, and liquid delivery. Finite element analysis results used to maximize jaw force are presented. A novel extension–retraction method used in the cautery tool is discussed. The liquid delivery payload features a novel storage and delivery mechanism combined with a mixing chamber for applying liquids such as dual-component fibrin sealants. Finally, *in vivo* results demonstrate for the first time the ability of operators to use these robots simultaneously to directly assist one another performing tasks in the abdominal cavity. Fundamental surgical tasks are demonstrated such as the control of hemorrhaging from a severed blood vessel, the dissection and cauterization of tissue, and the potential of delivering therapeutic drugs to a specified site. To the authors' knowledge, this is the first demonstration of performing these types of tasks from a wheeled robot.

II. Wireless Mobile Robot Platform

Our previous research focused on the design and development of a modular robotic platform with payloads to support several different surgical tasks. Extensive details of this work are presented in [17]. A summary of the key design features of this robot platform, which are incorporated into our current study, is presented in the following.

Stereolithography prototyping techniques are used to construct the housing components and wheels out of FullCure 720 Transparent material using an Objet Eden 350 3D printer. The inner housing consists of two halves. One half houses a control board consisting of an RF transceiver, a multichannel motor driver, and microprocessor control unit. Individual payloads are housed in the other half. Telemetry, communication, and

Manuscript received November 10, 2011; revised March 5, 2012, May 4, 2012, and July 25, 2012; accepted July 28, 2012. Date of publication August 8, 2012; date of current version September 14, 2012. This work was supported in part by the National Institutes of Health under Grant EB005663-01A1. *Asterisk indicates corresponding author*.

*J. A. Hawks is with the Department of Mechanical and Materials Engineering, University of Nebraska, Lincoln, NE 68566 USA (e-mail: jhawks2@unl.edu).

J. Kunowski was with the Department of Mechanical Science and Engineering, University of Illinois at Urbana-Champaign, Urbana, IL 61801 USA (e-mail: jacob.kunowski@gmail.com).

S. R. Platt is with the Department of Mechanical Science and Engineering, University of Illinois at Urbana-Champaign, Urbana, IL 61801 USA (e-mail: srplatt@illinois.edu).

Color versions of one or more of the figures in this paper are available online at http://ieeexplore.ieee.org.

Digital Object Identifier 10.1109/TBME.2012.2212439

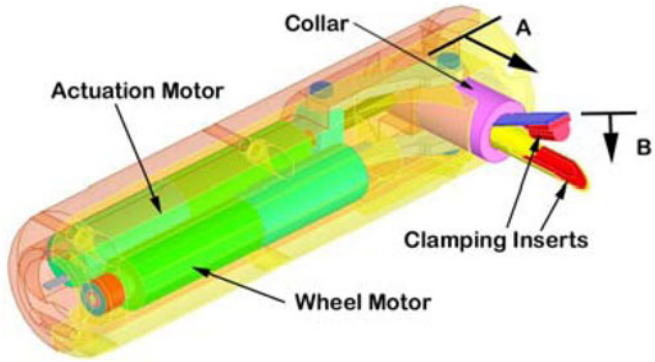

Fig. 1. Isometric view of CAD model illustrating the components of the clamping payload half of the robot. The control board, battery, and other wheel motor are located in the other half of the robot (not shown).

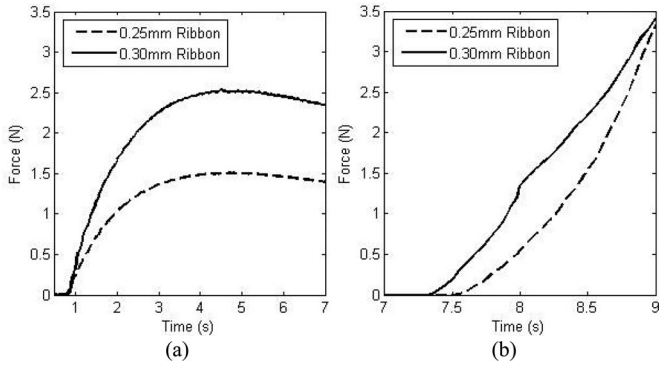

Fig. 2. Abaqus simulation results of the (a) required actuation force and (b) approximate jaw force for a 0.25- and 0.30-mm-thick ribbon.

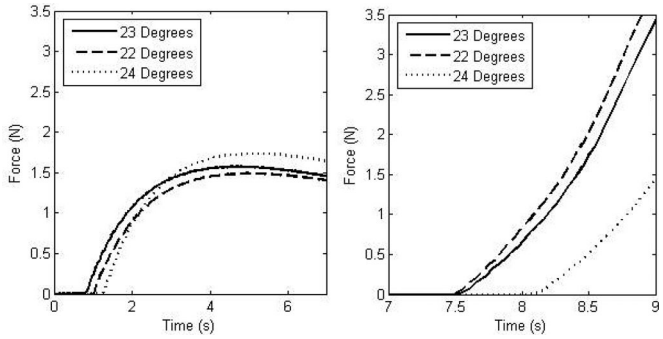

Fig. 3. Abaqus simulation results of the (a) required actuation force and (b) approximate jaw force for a 22°, 23°, and 24° ribbon profile angle.

the main control board are powered using a 185 mAh Tadiran TLM-1520MP lithium organic cell battery. Wheels slide over the inner housing to provide forward, backward, and turning motions. These wheels are 20 mm in diameter with nine helical grousers, 1.5 mm deep, arranged in a corkscrew pattern, and are powered by 6-mm permanent magnet direct current (PMDC) motors. The overall length of the robot platform is 100 mm. Multiple robots can be controlled simultaneously on different RFs. The wireless communication is built around a Nordic nRF2401 A 2.4-GHz ISM band single-chip radio transceiver, which has 125 addressable receive/transmit channels, and is connected to a 50-Ω chip antenna (LINX ANT-2.45-CHP). The ability of the robot platform to wirelessly measure physiological data in real-time, collect tissue samples, manipulate organs, and provide visual feedback was previously demonstrated *in vivo* using a porcine model [17].

III. New Payload Designs for Robotic Platform

A. Clamping Payload

Many laparoscopic procedures (e.g., cholecystectomy and hysterectomy) involve the clamping of vessels or other ducts during dissection or removal. The newly designed clamping payload reported here replaces the biopsy grasper previously reported in [17] that used plastic clamping inserts. Fig. 1 shows a schematic of the clamping payload. A 6-mm PMDC actuation motor with a 1064:1 reduction moves a lead screw linkage that allows a stainless steel collar to translate (direction A). As the collar moves outward, the clamping jaws close together. The top jaw is constructed of Nitinol ribbon, which flexes (direction B) as the collar moves. Nitinol is a superelastic alloy and can be flexed repeatedly without the potential for damage due to work hardening. Nitinol is also an accepted biomaterial widely used in stents and other devices. The bottom jaw remains stationary and provides a rigid base against which the top jaw can apply pressure for clamping.

The clamping inserts are smooth and rounded to reduce vascular damage caused by traditional clamping devices such as the mosquito clamp. The ribbed surface of the mosquito clamp causes regions of stress concentrations on tissue. Famaey [19] *et al*. found that patient trauma and recovery times are reduced when using smooth clamps compared to mosquito clamps.

Abaqus finite element software was used to investigate the effects design parameters, such as ribbon thickness and profile angle, had on actuation and jaw force without increasing the payload size [18]. The model was validated using experimental measurements of the actuation force needed to close the jaws [17]. A displacement boundary condition was used to translate the collar the maximum distance allowed by the payload dimensions. Two ribbon thicknesses, 0.25 and 0.30 mm, were readily available, and these were used for the numerical and experimental tests. Fig. 2 shows both ribbons produced approximately the same jaw force (3.4 N). However, the 0.25-mm ribbon required 40% less actuation force.

The ribbon profile angle was varied from 21° to 25° to investigate the relationship between the jaw opening width and the force produced [18]. Fig. 3 shows the Abaqus results of the 22°, 23°, and 24° profile. The force for the 24° profile is significantly less than the other simulations because the mechanical translation limit of the collar prevents the jaw from fully closing for profiles greater than 23°. Fig. 3 also shows similar actuation and jaw forces for the 22° and 23° profiles. Based on these results, a prototype was constructed using 0.25-mm Nitinol ribbon with a profile angle of 23°, which is expected to yield the most desirable combination of clamping force and jaw opening size (approximately 9 mm) without increasing the payload size.

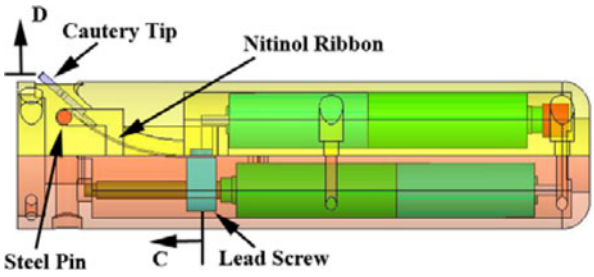

Fig. 4. Side view of CAD model illustrating the components of the cautery payload half of the robot.

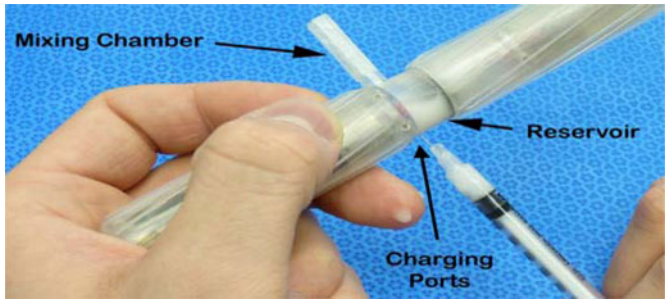

Fig. 5. Liquid delivery prototype being filled with needle and syringe.

B. Cautery Payload

The dissection of tissue, arteries, and other anatomical features such as the bile duct is common during laparoscopic surgery. The cautery payload must fit within the available payload space, heat to a temperature sufficient for cauterizing tissue, and retract within the payload during insertion. The cautery payload tip was constructed using a high-temperature cautery tip (Bovie Medical). Because the cautery tip is easy to bend, a retractable arm was designed to protect the tip during robot insertion and removal. As the lead screw translates (direction C), the actuation arm, constructed from Nitinol ribbon, extends (direction D) from the robot housing. The Nitinol ribbon shown in Fig. 4 is profiled using a shape-setting heat treatment [18]. The ribbon is held in the desired shape while heated at 500 °C for 10 min. After water quenching, the Nitinol ribbon maintains the curved profile.

The curved profile of the ribbon is designed so that the ribbon remains in contact with a stainless steel pin when the cautery tip is retracted. The pin provides a rigid base for the Nitinol ribbon to flex against during extension. When fully extended, the cautery tip is approximately 10 mm away from the robot housing, a sufficient length to easily contact tissue. The lead screw motion controls the ribbon flexure, and provides a few millimeters of motion along the axial direction of the robot. Wheel rotation provides gross robot movement in the transverse direction.

The cautery payload currently requires its own power source to sufficiently heat the cautery tip. The 185-mAh robot battery lacks the capacity to power both the cautery and onboard electronics for more than a minute. Therefore, a battery pack tethered to the main robot body powers the cautery with two AA alkaline batteries (1800 mAh). This battery pack was able to continuously power the cautery tip for over 15 min during laboratory testing. The voltage losses in the tether were experimentally measured to be 200 mV. The cautery tip temperature was experimentally measured at 1035 °C using a thermocouple. Similarly, the original Bovie Medical high-temperature disposable cautery was experimentally measured to have tip temperature of approximately 1200 °C.

Power to the cautery tip is controlled by the opening and closing of a PVN012A series photovoltaic relay switch, which is also contained in the battery pack. The relay itself is controlled by a digital output signal from the main control board of the robot.

C. Liquid Delivery Payload

Tissue sealants are becoming more prominent in conventional and laparoscopic surgery. Liquid hemostatic compounds such as BioGlue and Evicel have been used in conventional and MIS as adjuncts or replacements for hemostatic techniques that require extensive training, such as suturing and knot tying [20]–[22]. Another advantage of tissue sealants is avoiding the nerve damage and chronic pain that sometimes accompanies the use of staples or tacks [23]–[25]. Unmanageable bleeding during MIS is the most common indication for reverting to traditional open surgery [25]. Delivering liquid compounds from an *in vivo* robot could potentially limit the need for a surgeon to revert to open surgery.

A robot has several requirements if it will carry a liquid payload. First, it must have a liquid-tight chamber. If the payload is a dual-component fibrin sealant such as Evicel, the chamber must be capable of storing the two different liquids separately. Second, if the payload has dual components that must be mixed, a mixing chamber must be designed and incorporated into the robot to sufficiently mix the two liquids before they are dispensed. Finally, an actuation mechanism is needed to force the liquids through the mixing chamber, dripping them directly onto the tissue surface. A brief summary of the design of the liquid delivery robot is presented in the following. An extensive discussion of the design and the results of *ex vivo* laboratory testing can be found in [26].

A region in the modular platform payload area is first hollowed out to create a sealed chamber for liquid storage. A syringe-like plunger is designed to seal the chamber from the rest of the robot. A PMDC motor is used to actuate the plunger using a lead screw mechanism. The liquid is expelled from the chamber through small exit ports. The plunger is split into two semicircular heads, allowing it to slide over a center divider. The center divider bisects the chamber, creating two separate storage volumes. The split design also prevents rotation of the plunger, constraining its motion to translation only.

The payload body has two charging ports, 0.35 mm in diameter. To charge an empty robot, a 30-gage needle and syringe is used to inject the liquid into the reservoir once the robot is fully assembled, as shown in Fig. 5. The maximum usable volume of liquid is 1.7 mL, comparable to a standard 2.0-mL package of Evicel [27].

A mixing chamber was also designed and incorporated into the robot to accommodate dual components, such as tissue

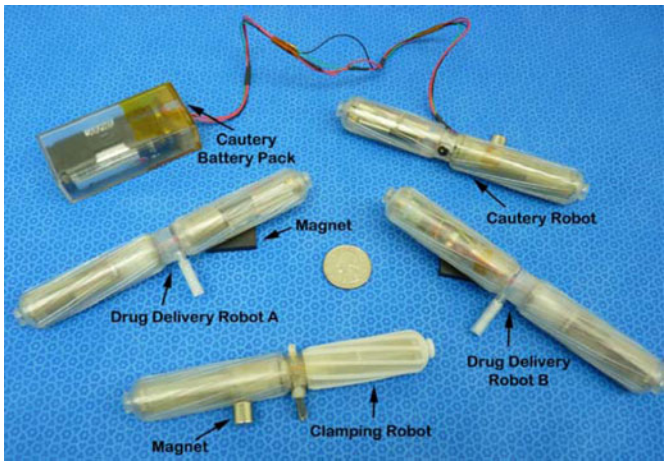

Fig. 6. Wireless mobile robots prior to insertion.

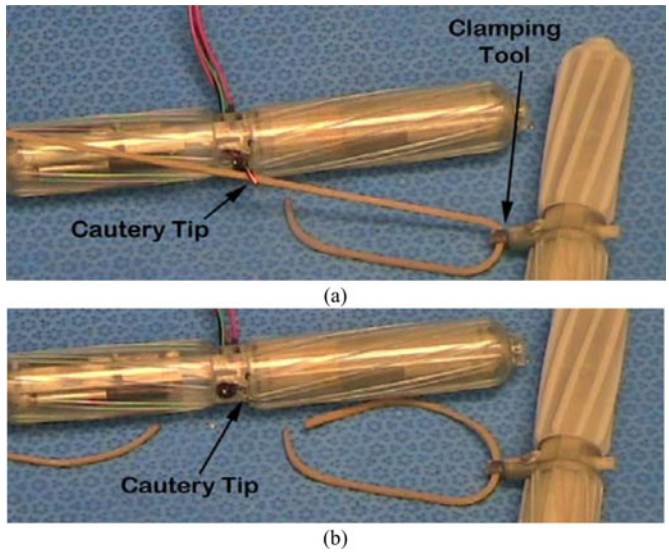

Fig. 7. (a) Laboratory experiments showing a "stretch and dissect" demonstration with multiple robots. (b) After the rubber band is dissected, the cautery tip is retracted.

sealants, that require mixing. This does not limit dispensing a single type of liquid from one or both chambers as long as they do not damage the robot housing and fit within the viscosity limitations [26]. The internal structure of the mixing chamber was built directly into the payload body using a stereolithography rapid prototyping technique. This chamber extends from the body of the robot, and functions as both a mixing device and a hose that facilitates accurate delivery of one- or two-component liquids.

The internal structure of the mixing chamber was designed using analyses of static mixers from the literature and computational fluid dynamic simulations using ANSYS FLUENT [26]. The simulations were validated using a color dilution method during laboratory tests. During the exploration of different designs using simulation, a mixing efficiency of 67% was achieved using two liquids that differ in viscosity by a factor of 30 (properties similar to fibrin-type sealants), through a chamber only 4.0 mm high, 2.8 mm wide, and 18.0 mm long. It was also shown that the degree of mixing can be increased to 90% by lengthening the chamber to 36.0 mm.

IV. Laboratory Experiments

Laboratory experiments were conducted to demonstrate communication and functional repeatability before *in vivo* demonstrations. These demonstrations serve as a proof of concept for these devices. Fig. 6 [18] shows the robot prototypes prior to the laboratory experiments. The control interface features two joysticks (one for each wheel), a bidirectional switch for the actuation motor, and an ON/OFF switch for the cautery. The simultaneous use of two robots requires two controllers. If simultaneous operation is unnecessary, a single operator can operate multiple robots by switching between controls.

A normally closed Hall effect ON/OFF switch was added to the main control board. When the magnets in Fig. 6 are removed, the robots are powered on. Laboratory experiments showed that magnets attached to the robots for more than two months did not affect the functionality of the PMDC motors or any other robot component.

Another laboratory experiment used two operators to "stretch and dissect" a rubber band with the clamping and cautery robots. The robots were initially placed approximately 30 cm away from the rubber band for each demonstration, and the initial orientation of the robots varied from experiment to experiment. Once the clamping robot pulled the rubber band tight, the cautery robot was positioned so that the rubber band could be cut (see Fig. 7) [18]. This experiment was performed successfully without operator intervention five times out of six attempts. The single failure occurred during the initial attempt when the rubber band was not completely secured within the clamping jaws. Each successful demonstration required less than 5 min to complete with approximately 70% of the time used to position the rubber band within the clamping jaw.

V. *In Vivo* Demonstrations

In vivo robot performance was demonstrated under an Institutional Animal Care and Use Committee approved protocol using porcine models. Demonstrating the feasibility of these robots to perform *in vivo* tasks is needed before systematic performance testing takes place. The female swine is generally used for laparoscopic surgical training because the size and internal anatomy of the abdominal cavity closely resemble human anatomy. Several *in vivo* surgical tasks were performed for the first time using these robots. These experiments demonstrated the robots' abilities to successfully clamp a blood vessel, cauterize a wound, and accurately dispense a liquid during an *in vivo* procedure. Two additional *in vivo* procedures demonstrated multiple robots executing surgical tasks. All three wireless robots were inserted through a single incision. Demonstrating the mobility of the robot continued to build upon the successful results of previous *in vivo* tests [17].

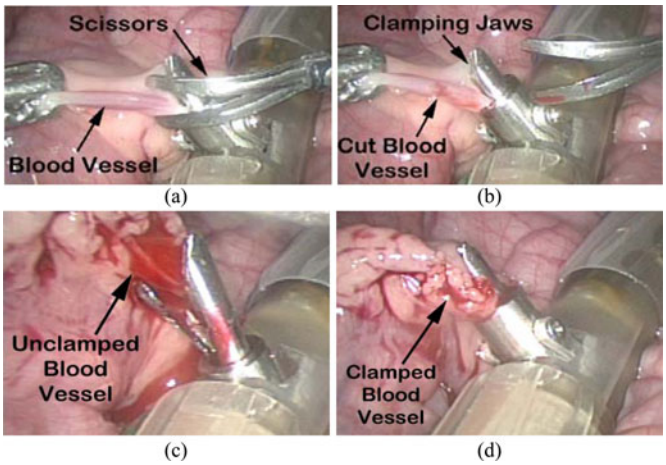

Fig. 8. *In vivo* laparoscope images showing (a) the cutting of a blood vessel, and (b) the successful clamping resulting in no extensive bleeding. Extensive bleeding (c) occurs when the blood vessel is unclamped, and (d) stops when the clamping jaws are closed again.

A. In Vivo Clamping of a Blood Vessel

The first test performed to demonstrate *in vivo* functionality of the clamping payload consisted of a robot being directed to a blood vessel location, clamping to one of the intestinal branches of the mesentery artery, dissecting the vessel while remaining clamped, and observing if any leakage occurred. Assistance from a surgeon was needed to position the robot because of a wheel malfunction; however, the mobility needed to clamp is very similar to the mobility demonstrated previously in the collection of biopsy samples [17]. During this procedure, a surgeon manually positioned the blood vessel inside the clamping jaws. Images from the laparoscope are shown in Fig. 8 [18].

After the robot clamped the blood vessel, a surgeon manually dissected it [see Fig. 8(a)]. With the robot continuing to clamp and hold the blood vessel, no hemorrhaging occurred after it was cut [see Fig. 8(b)]. Upon opening the clamping jaws, blood flowed freely. Finally, with blood flowing into the actuation mechanism [see Fig. 8(c)], the clamping jaws were again closed and sufficient pressure was applied to the blood vessel to restore hemostasis [see Fig. 8(d)]. The assistance provided by the robot eliminated the need for a surgeon to manipulate two tools simultaneously during the clamp and dissect procedure.

B. In Vivo Cautery

To demonstrate robotic *in vivo* cautery functionality, a wireless mobile robot equipped with a cautery payload was inserted into the abdominal cavity and used to cauterize a wound on the spleen. The robot was successfully maneuvered to the site of the wound without any direct manipulation by a surgeon. Once the wound was located, the cautery tool was extended and applied to the injury site.

Laparoscopic images taken during the *in vivo* tests are shown in Fig. 9 [18]. The tip of the cautery tool on the mobile robot is shown, applied to the wound in Fig. 9(a). Once activated, fine movements of the robot were used to cauterize a large enough area of the wound to achieve hemostasis. The cauterized area is shown in Fig. 9(b).

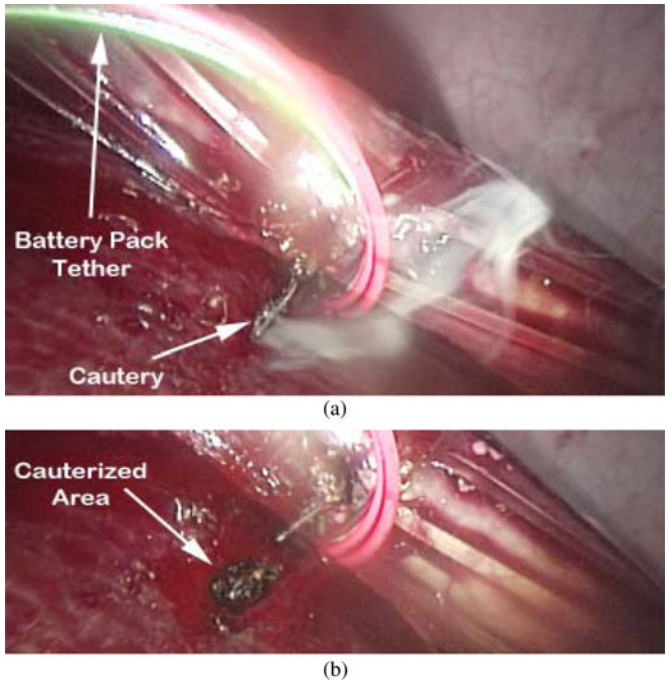

Fig. 9. *In vivo* laparoscopic images of (a) the cautery payload cauterizing a bleeding wound on the spleen, and (b) after the spleen is cauterized.

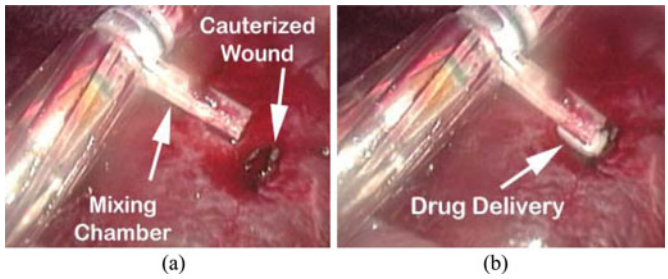

Fig. 10. *In vivo* images of (a) the liquid delivery robot approaching an injured area of the spleen, and (b) delivering a white liquid directly into a wound.

A surgeon was then able to wirelessly maneuver the robot to a second location on the spleen and repeat the cauterization process. Once hemostasis was achieved, the cautery tool was retracted, and the robot was directed to another region in the abdominal cavity for further testing and subsequent removal.

C. In Vivo Liquid Delivery

A third functionality test demonstrated *in vivo* operation of the liquid delivery payload by inserting a robot equipped with a liquid delivery payload into the abdominal cavity and then directing it to multiple sites at each of which it dispensed liquid. A mixture of white paint and water was used to create a liquid that had a clear color contrast with the internal organs and tissue.

The liquid delivery robot was used to successfully dispense liquid at two different sites located on the injured spleen. Fig. 10 [18] shows an image from the laparoscope video demonstrating the robotic device dispensing the liquid directly onto the

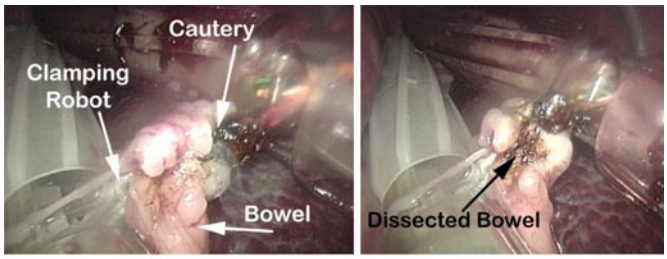

Fig. 11. *In vivo* laparoscopic images showing (a) the clamping robot holding a piece of the small intestine (or bowel), while the cautery robot dissects the small intestine. (b) Cauterized area shown after a partial dissection is finished.

cauterized wound discussed in the previous section. Wireless control of the plunger allows a surgeon to dispense liquid at multiple locations, and regulate the amount of liquid delivered. The robot could be maneuvered to multiple sites without directly manipulating it. The *in vivo* delivery of the liquid directly onto two different cauterized wounds was successful.

D. In Vivo Cooperative Tasks

After successful individual *in vivo* testing of clamping, cautery, and liquid delivery payloads, the two robots equipped with clamping and cautery payloads were used for a single cooperative "stretch and dissect" demonstration. This test demonstrated the robots working together *in vivo* to complete surgical tasks that require the simultaneous manipulation of more than one tool. Two operators were used to operate the robots. The clamping robot grasped a portion of the small intestine (bowel), while the cautery robot was used to cut a portion of the intestine near the grasping site (Fig. 11) [18]. Fine movements from both robots were used to completely dissect the bowel without any direct assistance from traditional laparoscopic tools. The "stretch and dissect" task required nearly 10 min to complete. Approximately half of this time was needed to direct the robots into position; the other half was needed to complete the grasping and dissection. The laparoscope was used for visualization, but no other surgical tools were inside the abdominal cavity during the test.

It should be emphasized also that the *in vivo* demonstration of liquid delivery, discussed in the previous section, was also an example of using two robots sequentially to perform surgical tasks. In this case, the cautery robot first cauterized the injured spleen. Then, the liquid delivery robot was maneuvered to the injury site to dispense liquid onto the cauterized region. Both of these tasks were completed without any direct intervention from a surgeon.

VI. Discussion

These devices demonstrate the feasibility of placing several miniature robots inside the abdominal cavity through a single incision and using them together to perform surgical tasks. *In vivo* cooperation between multiple robots expands the capabilities and potential of these types of robots. Fundamental tasks such as "stretch and dissect" maneuvers are possible using these robots. The mobility of the robots ensures that the location of the incision is not necessarily confined to relatively close proximity to the surgery site, as it is in conventional laparoscopic surgery.

The performance of the clamping payload could be improved by selecting a lower gear reduction for the actuation motor. Surgeons desire a clamping mechanism that responds quickly, and the current actuation time of 9 s must be reduced. The high gear reduction was selected to maximize the torque produced by the motor in order to overcome unknown resistive forces that may be encountered *in vivo*. It is common for biological matter (i.e., tissue, blood, and membrane) to infiltrate the actuation mechanism. Additional ribbon thicknesses must be tested and thoroughly evaluated for an optimization analysis of the applied clamping force. Famaey *et al.* [19] also suggest that more experiments with different clamping durations, speeds, and recovery periods should be performed to help evaluate the effect that clamping for long time periods has on tissue healing and patient recovery. The versatile robot described here can apply the desired speed and pressure repeatedly for such tests more accurately than a surgeon, making these studies feasible *in vivo*.

The use of a tethered power source for the cautery payload demonstrated that a mobile robot can perform surgical tasks using a cautery device. Battery pack prototypes could be magnetically attached to the inside of the abdominal wall, allowing a surgeon to position it from outside the patient with a magnetic handle similar to one used on a previously developed robotic camera payload [17]. Improvements in battery performance could allow the cautery power source to be incorporated into the body of the robot itself, eliminating the need of a secondary battery pack and the additional tethers.

This study demonstrates the feasibility of developing a liquid delivery payload that could be used for a variety of therapeutic compounds. Simulations have shown that mixing efficiencies up to 90% are readily achievable.

It is challenging to navigate within the abdominal cavity due to obstacles such as internal organs. Fluids and tissues also make it difficult to maintain sufficient traction for wheeled mobility. Because *in vivo* mobility challenges were addressed in our previous work [17], those results were not discussed here. These challenges have the most influence on the time needed for these demonstrations, which required approximately 3.5 min to direct the robots into position.

The *in vivo* demonstrations presented are a potential step toward using these robots to assist with more complex procedures that are commonly performed during laparoscopy. Our previous work [17] did not demonstrate robots such as these assisting each other by directly performing sequential or cooperative surgical tasks on the same injured tissue. Prototypes meeting the design goals for a clamping, cautery, and liquid delivery robot were met. Each of these robots performed successful *in vivo* proof-of-concept demonstrations of clamping a blood vessel, cauterizing a wound, and delivering a liquid to a wound. Finally, the clamping and cautery robots were used to cooperatively perform a "stretch and dissect" procedure on bowel tissue.

VII. Future Directions

Systematic testing on various design parameters is needed over a greater range of experimental parameters. Follow-up experiments using lower actuation gear ratios will investigate the reliability of faster clamping mechanisms using less motor torque. Likewise, the clamping insert geometry, cautery efficiency, and liquid mixing efficiency will undergo systematic testing to ensure a robust design. Experiments will also be conducted to compare the speed, accuracy, and repeatability of the robot with a surgeon using laparoscopic tools. Thorough experimental evaluation beyond visual demonstration is a necessary step in the demonstration of performing entire surgical procedures rather than fundamental tasks.

Acknowledgment

The authors would like to thank Dr. D. Oleynikov from the University of Nebraska Medical Center, Dr. S. Farritor from the University of Nebraska, and Drs. J. Schoen and M. Rentschler from the University of Colorado for their assistance during *in vivo* testing.

References

[1] M. J. Mack, "Minimally invasive and robotic surgery," *J. Amer. Med. Assoc*., vol. 285, no. 5, pp. 568–572, 2001.

[2] A. Cuschieri, "Technology for minimal access surgery," *Brit. Med. J*., vol. 319, pp. 1–6, 1999.

[3] F. Tendick, S. S. Sastry, R. S. Fearing, and M. Cohn, "Applications of micromechatronics in minimally invasive surgery," *IEEE/ASME Trans. Mechatronics*, vol. 3, no. 1, pp. 34–42, Mar. 1998.

[4] V. Kim, W. Chapman, R. Albrecht, B. Bailey, J. Young, L. Nifong, and W. Chitwood, "Early experience with telemanipulative robot-assisted laparoscopic cholecystectomy using da Vinci," *Surg. Laparosc., Endosc. Percutan. Tech*., vol. 12, no. 1, pp. 33–40, 2002.

[5] T. Lafullarde, D. I. Watson, G. G. Jamieson, J. C. Myers, P. A. Game, and P. G. Devitt, "Laparoscopic Nissen fundoplication: Five-year results and beyond," *Arch. Surg*., vol. 136, pp. 180–184, 2001.

[6] T. J. Heikkinen, K. Haukipuro, S. Bringman, S. Ramei, A. Sorasto, and A. Hulkko, "Comparison of laparoscopic and open Nissen fundoplication 2 years after operation: A prospective randomized trial," *Surg. Endosc*., vol. 14, pp. 1019–1023, 2000.

[7] G. H. Ballantyne, "Robotic surgery, telerobotic surgery, telepresence, and telementoring. Review of early clinical results," *Surg. Endosc*., vol. 16, pp. 1389–1402, 2002.

[8] F. Corcione, C. Esposito, D. Cuccurullo, A. Settembre, N. Miranda, F. Amato, F. Pirozzi, and P. Caiazzo, "Advantages and limits of robot-assisted laparoscopic surgery: Preliminary experience," *Surg. Endosc*., vol. 19, no. 1, pp. 117–119, 2005.

[9] K. Moorthy, Y. Munz, A. Dosis, J. Hernandez, S. Martin, F. Bello, T. Rockall, and A. Darzi, "Dexterity enhancement with robotic surgery," *Surg. Endosc*., vol. 18, pp. 790–795, 2004.

[10] S. DiMaio, M. Hanuschik, and U. Kreaden, "The da vinci surgical system," in *Surgical Robotics: Systems Applications and Visions*. New York: Springer, 2011, ch. 9, pp. 199–217.

[11] G. F. Dakin and M. Gagner, "Comparison of laparoscopic skills performance between standard instruments and two surgical robotic systems," *Surg. Endosc*., vol. 17, pp. 574–579, 2003.

[12] D. Nio, W. A. Bemelman, K. T. den Boer, M. S. Dunker, D. J. Gouma, and T. M. van Gulik, "Efficiency of manual versus robotical (Zeus) assisted laparoscopic surgery in the performance of standardized tasks," *Surg. Endosc*., vol. 16, pp. 412–145, 2002.

[13] K. Harada, E. Susilo, A. Menciassi, and P. Dario, "Wireless reconfigurable modules for robotic endoluminal surgery," in *Proc. IEEE Int. Conf. Robot. Autom*., May 2009, pp. 2699–2704.

[14] M. Piccigallo, U. Scarfogliero, C. Quaglia, G. Petroni, P. Valdastri, A. Menciassi, and P. Dario, "Design of a novel bimanual robotic system for single port laparoscopy," *IEEE/ASME Trans. Mechatronics*, vol. 15, no. 6, pp. 871–878, Dec. 2010.

[15] T. D. Wortman, K. W. Strabala, A. C. Lehman, S. M. Farritor, and D. Oleynikov, "Laparoendoscopic single-site surgery using a multifunctional miniature *in vivo* robot," *Int. J. Med. Rob. Comput.-Assisted Surg*., vol. 7, no. 1, pp. 17–21, 2011.

[16] J. Ding, K. Xu, R. E. Goldman, P. Allen, D. Fowler, and N. Simaan, "Design, simulation and evaluation of kinematic alternatives for insertable robotic effectors platforms in single port access surgery," in *Proc. IEEE Int. Conf. Robot. Autom*., May 2010, pp. 1053–1058.

[17] S. R. Platt, J. A. Hawks, and M. E. Rentschler, "Vision and task assistance using modular wireless *in vivo* surgical robots," *IEEE Trans. Biomed. Eng*., vol. 56, no. 6, pp. 1700–1710, Jun. 2009.

[18] J. A. Hawks, "Improved mobile wireless *in vivo* surgical robots: Modular design, experimental results, and analysis," Ph.D. dissertation, Dept. Mech. Eng., Univ. Nebraska, Lincoln, 2010.

[19] N. Famaey, E. Verbeken, S. Vinckier, B. Williaert, P. Herijgers, and J. V. Sloten, "*In vivo* soft tissue damage assessment for applications in surgery," *Med. Eng. Phys*., vol. 32, pp. 437–443, 2010.

[20] L. A. Evans and A. F. Morey, "Hemostatic agents and tissue glues in urologic injuries and wound healing," *Urologic Clin. North Amer.*, vol. 33, no. 1, pp. 1–12, 2006.

[21] T. W. Jarrett, D. Y. Chan, T. C. Charambura, O. Fugita, and L. R. Kavoussi, "Laparoscopic pyeloplasty: The first 100 cases," *J. Urol*., vol. 167, no. 3, pp. 1253–1256, 2002.

[22] W. K. Johnston, J. S. Montgomery, B. D. Seifman, B. K. Hollenbeck, and J. S. Wolf Jr., "Fibrin glue v sutured bolster: Lessons learned during 100 laparoscopic partial nephrectomies," *J. Urol*., vol. 174, no. 1, pp. 47–52, 2005.

[23] A. C. Hindmarsh, E. Cheong, M. P. N. Lewis, and M. Rhodes, "Attendance at a pain clinic with severe chronic pain after open and laparoscopic inguinal hernia repairs," *Brit. J. Surg*., vol. 90, no. 9, pp. 1152–1154, 2003.

[24] N. Katkhouda, E. Mavor, M. H. Friedlander, R. J. Mason, M. Kiyabu, S. W. Grant, K. Achanta, E. L. Kirkman, K. Narayanan, and R. Essani, "Use of fibrin sealant for prosthetic mesh fixation in laparoscopic extraperitoneal inguinal hernia repair," *Ann. Surg*., vol. 233, no. 1, pp. 18–25, 2001.

[25] M. L. Saxton, "Hemostasis in minimally invasive liver surgery," *Surgery*, vol. 142, no. 4, pp. S46–S49, 2007.

[26] J. Kunowski, "Development of a liquid drug delivery payload for modular, wireless, incorporeal robots for laparoscopic surgery," M.S. thesis, Dept. Mech. Eng., Univ. Illinois, Urbana, 2010.

[27] "Evicel fibrin sealant (human)," Package Insert, Johnson & Johnson, Somerville, NJ, 2003

Jeff A. Hawks received the B.S. and M.S. degrees in mechanical engineering and the Ph.D. degree in engineering all from the University of Nebraska, Lincoln, in 2004, 2007, and 2010, respectively.

He was a Visiting Researcher in the Army Research Laboratory, Aberdeen, MD. He was also a Graduate Research Assistant in the Advanced Surgical Technologies Laboratory, University of Nebraska. He is currently a Research Assistant Professor in the Department of Mechanical and Materials Engineering, University of Nebraska, Lincoln. His current research interests include surgical robotics and medical devices, autonomous ground and air vehicles, agricultural robotics, mechatronics, and biomechanics.

Jacob Kunowski received the B.S. and M.S. degrees in mechanical engineering from the University of Illinois at Urbana-Champaign, Urbana, in 2008 and 2010, respectively.

Stephen R. Platt received the B.A. degree in physics and astronomy from Williams College, Williamstown, MA, in 1983, the M.S. and Ph.D. degrees in astronomy and astrophysics from the University of Chicago, Chicago, IL, in 1984 and 1991, respectively, and the M.S. degree in mechanical engineering from the University of Nebraska, Lincoln, in 2003.

He was a Farr Research Fellow and a NASA Graduate Research Fellow at the University of Chicago. He was a Research Associate Professor in the Department of Mechanical Engineering, University of Nebraska, Lincoln. He was also a Postdoctoral Research Associate at Princeton University, Princeton, NJ. He is currently a Research Associate Professor in the Department of Mechanical Science and Engineering, University of Illinois at Urbana-Champaign, Urbana. His current research interests include biomedical sensors, surgical robotics and medical devices, mechatronics, and instrument development for astrophysics applications.